eJSE International

Electronic Journal of Structural Engineering 11(1) 2011

Global Buckling Experiments on Sandwich Columns with Soft Shear Cores

Mario M. Attard
School of Civil and Environmental Engineering
The University of New South Wales, Sydney 2052, Australia

Email: m.attard@unsw.edu.au

ABSTRACT: Several failure modes for sandwich columns under compression are said to be possible with shear crimping or shear buckling suggested for short columns with soft shear cores. The buckling formulas and theoretical assumptions of Engesser and Haringx for isotropic columns and soft shear core sandwich columns are reviewed. An important distinction is made between the isotropic column buckling formula attributed to Haringx and the theoretical assumptions underpinning his approach. It is shown that the theoretical approaches of Haringx and Engesser yield the same basic buckling equation for soft shear core sandwich columns when the thickness is very small in comparison to the core thickness, and the shear in the face sheets, the axial force in the core and the bending within the face sheets are ignored. To determine whether shear crimping (shear buckling) is a member or localised type of buckle, tests on low slenderness - short sandwich columns identified as possibly exhibiting shear crimping, were preformed. The test specimens were constructed from 10 mm thick Divinycell H45, H80, H100 and H200 foam for the core and 1 mm face sheets made of Aluminum 2024-T3. The lengths of the columns varied from 20 to 500 mm. The columns were end-clamped according to ASTM C 364-99 [1] and placed in a servo-controlled compression testing machine. The width of the specimens was 100 mm and two specimens at each length were tested. The adhesive chosen was a toughened epoxy, trade name “Devcon Epoxy Plus". Measurements of the mid-span lateral displacement were used in a Southwell type plot to determine the elastic global buckling load. The shear modulus of the core was determined from three point bending tests according to ASTM-C-393 [2]. Some of the very short specimens failed with buckling of the face sheet within the clamped region. None of the tests exhibited shear crimpling or shear buckling modes and the global buckling loads for very short columns were much higher than the shear buckling limit of Engesser. Wrinkling failure was not considered.

Keywords: Column Buckling, Buckling Experiments, Sandwich Columns, Shear Buckling, Shear Deformations

1 INTRODUCTION

Shear deformations are important considerations in the elastic buckling analysis of the compressive strength of sandwich columns. Engesser [3-4] and later Haringx [5] extended Euler’s column buckling formula for prismatic straight columns made of an isotropic material by including shear deformations. Engesser’s formula predicts an upper limit sometimes referred to as the shear buckling load as the slenderness is reduced. Haringx [5] derived an alternate buckling formula which predicted an infinite buckling load as the slenderness approached zero. Haringx’s formula when modified to take account of axial deformations prior to buckling agreed well with the experimental results for short rubber rods and helical springs. For the helical springs, the experimental results showed that for small slenderness, springs do not buckle below a slenderness of about 4.9. This observation agreed with the Haringx’s formula but not with Engesser’s which predicted buckling for any slenderness. Ziegler [6] incorporated axial, as well as, shear deformations and derived a modified Engesser formula. Ziegler’s modified Engesser formula predicts a limit for the slenderness below which there is no buckling and for isotropic prismatic columns does not have the upper limit of GA as in the unmodified Engesser formula. Ziegler’s modified Engesser formula compared well with the buckling of rubber rods but did

not match the experimental results for helical springs (see [7]). Engesser and Haringx used different definitions for the beam force internal actions: the shear force Q and the axial force N. Each approach assumes a different orientation for the beam force internal actions (see Figure 1). Engesser assumed the axial force to be tangential to the centroidal axis while the shear force was taken as perpendicular. Haringx assumed that the axial force was normal to the cross-sectional plane and the shear force perpendicular to the plane. Reissner [8] supported Haringx's approach and definition of internal actions.

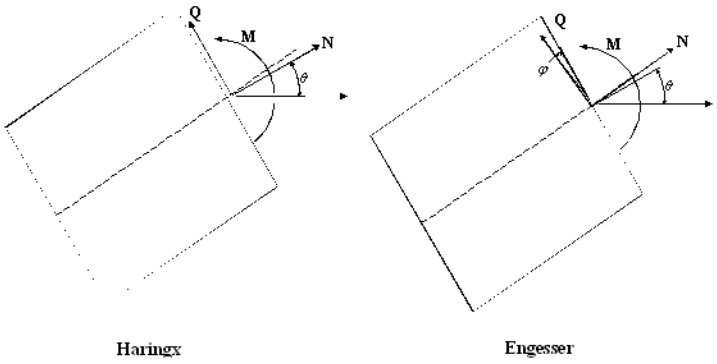

Figure 1 Engesser and Haringx Beam Actions

There has been a continuing debate in the literature about firstly whose buckling formula is correct, and secondly about whose theoretical approach for the internal beam force actions is correct (see refs [6-23]). Related to this debate is the question about the correct finite strain constitutive relationship for linearly elastic isotropic materials. When reviewing the buckling capacity of sandwich columns (see Figure 2) with weak cores, Bazant & Beghini [15-16] found that Engesser's formula gave a reasonable match to the experimental results of Fleck and Sridhar [24] and concluded that Engesser's column buckling formula was correct for sandwich columns with weak cores (see Figure 3). In Figure 3, P_{cr} is the elastic critical load, P_{euler} is the Euler buckling load and G_cA_m is a so-called localized "shear buckling load" (G_c the shear modulus and A_m the effective core shear area). Fleck and Sridhar tested 15 sandwich columns with soft shear cores in compression with 9 columns observed to fail by core shear macrobuckling or shear crimping. The test specimens were constructed from Divinycell H30, H100 and H200 foam for the core and face sheets made from 4 layers of eight harness satin weave 7781 E-glass fibres. The experimental results of Fleck and Sridhar [24] are compared to Engesser's formula Eq. (1) in Figure 3. At very small column lengths (above 10), it is seen that Fleck and Sridhar's results congregate about the shear buckling GA_m prediction.

The work by Attard and Hunt [11] supported Haringx's "theoretical approach" and Reissner's [8] definition for beam internal force actions. Attard and Hunt [11] derived a buckling formula for sandwich columns using a consistent hyperelastic constitutive relationship for the face sheets and core of a sandwich column. The sandwich column buckling formula by Attard and Hunt [11] was derived using a theoretical approach consistent with Haringx's and was almost the same as the formula derived using Engesser's approach. Why does Engesser and Haringx's theoretical approach yield the same result for sandwich columns with thin face sheet and very soft shear cores? For a sandwich column with very thin face sheets , in which we assume no shear deformations in the face sheets and the axial force acting on the face sheets is in the same direction as the centroidal axis of the column then the theoretical approach of Engesser and Haringx yield the same terms for the face sheet. The core is very soft so if we ignore the axial force component within the core then the direction of the shear in the core whether perpendicular to the centroidal axis or parallel to the deformed plane of the core doesn't matter and therefore the orientation of the shear force doesn't matter and the theoretical approaches of Engesser and Haringx yield the same terms. So, for the situation where there is no shear in the face sheets, the face sheets take all the axial stress and the core basically only contributes by taking shear without axial stress/force, the two theoretical approaches of course give the same result. This will be demonstrated in detail in this paper by looking at the buckling equations for a sandwich column.

Haringx's column buckling formula was derived for a completely different physical problem to that for a sandwich column with a soft shear core. Haringx's column buckling formula is for a beam constructed out of a single isotropic material and is based on constant shearing through the full depth of the bending cross-sectional plane. Haringx's column buckling formula with an equivalent shear rigidity is not applicable to sandwich columns or to laced columns, columns with batten plates or with perforated cover plates and columns with open webs, where there is a zigzag shearing pattern of deformations through the cross-section. This does not mean that Haringx's theoretical approach and that of Reissner cannot be used for sandwich columns. Problems occur when a sandwich column with two materials (face sheet and core) is modeled by an equivalent column with a single effective bending and shear rigidity.

For sandwich columns, Allen [25] gives two buckling formulas quoted widely in the literature, for thin or thick face sheet sandwich columns:

Thin Faces:

$$\frac{P_{cr,Allen}}{G_c A_m} = \frac{\dfrac{P_{euler}}{G_c A_m}}{1+\dfrac{P_{euler}}{G_c A_m}} \quad A_m = A_c \frac{(c+t)^2}{c^2} \quad A_c = cb \qquad (1)$$

Thick Faces:

$$\frac{P_{cr,Allen}}{G_c A_m} = \frac{P_{face}}{G_c A_m} + \frac{\dfrac{P_{euler}}{G_c A_m} - \dfrac{P_{face}}{G_c A_m}}{1+\dfrac{P_{euler}}{G_c A_m} - \dfrac{P_{face}}{G_c A_m}} \qquad (2)$$

In Eq. (1), P_{face} is the Euler buckling capacity of the face sheets as independent struts while the thickness of the face sheets is denoted by t , the width of a sandwich section is taken as b and the core thickness is given by c (see Figure 2). The column buckling formula of Engesser is in essence the same as Allen's formula for thin faces, Eq. (1). The face sheet elastic modulus and shear modulus are denoted by E_f and G_f, respectively, while for the core they are denoted by E_c and G_c, respectively. Figure 4 shows three modes of possible buckling failure modes. The upper limit of Engesser's buckling formula is $G_c A_m$ which has been referred to as the shear buckling load. Shear buckling is sometimes referred to as "shear crimping" and is illustrated in Figure 4.

Shear crimping is shown as a localized failure. Vadakke and Carlsson [26] proposed that shear crimping is a form of face wrinkling or a localized postbuckling mode. Shear crimping can sometimes be initiated by a localized material failure.

As stated previously, Allen's formula for thin face sheets Eq. (1) is essentially the same as Engesser's formula. However, for a core weak in shear, as the slenderness is reduced, Eq. (2) rather than Eq. (1) is applicable for thin face sheets, as when the core ceases to provide effective connection between the faces, the face sheets buckle as independent struts. Hence, it could be concluded that there is no shear buckling upper limit for the critical load as the slenderness is reduced since in the limit P_{cr} approaches P_{face}.

Attard & Hunt [11] modeled the face sheets and core as two separate materials and using a finite strain hyperelastic constitutive model which was consistent with the beam action assumptions of Haringx [5], derived the following equation for the buckling of soft shear core sandwich columns:

$$\frac{P_{cr}}{G_c A_c} = \frac{P_{euler}}{G_c A_c}\left(1 - \frac{\dfrac{P_{euler}}{G_c A_c}\dfrac{r_c^4}{r^4}}{1+\dfrac{P_{euler}}{G_c A_c}\dfrac{r_{c2}^2}{r^2}}\right) \qquad (3)$$

In which:

$$EI_{tot} = 2E_f I_f + E_c I_c + 2E_f A_f \left(\frac{c+t}{2}\right)^2$$

$$r_c^2 = \frac{E_c I_c + 2E_f A_f \left(\dfrac{c}{2}\right)\left(\dfrac{c+t}{2}\right)}{EA_{tot}}$$

$$r^2 = \frac{EI_{tot}}{EA_{tot}} \quad A_f = bt \quad A_{tot} = 2A_f + A_c \qquad (4)$$

$$r_{c2}^2 = \frac{E_c I_c + 2E_f A_f \left(\dfrac{c}{2}\right)^2}{EA_{tot}} \quad I_f = \frac{bt^3}{12} \quad I_c = \frac{bc^3}{12}$$

Since $\dfrac{P_{face}}{P_{euler}} << 1$, Attard & Hunt [11] derived the following approximation to Eq. (3), that is:

$$\frac{P_{cr}}{G_c A_m} = \frac{\dfrac{P_{euler}}{G_c A_m}\left(1+\dfrac{P_{face}}{G_c A_m}\right)}{1+\dfrac{P_{euler}}{G_c A_m}} \qquad (5)$$

When the effective length of the column is relatively long $\dfrac{P_{face}}{G_c A_m}$ would be small and the above equation matches Eqs. (1), essentially Engesser's solution. However, if the slenderness is very small, the buckling load of the face sheets acting independently will dominate. For most practical sandwich column configurations with thin face sheets and weak cores, Eqs. (2) & (3) give solutions very close to those derived using Eq. (5). Figure 3 compares the predictions of Eq. (5) with the results of Fleck and Sridhar [24]. The comparison is reasonable except for very small column lengths ($P_{euler}/G_c A_m$ above 10), where Fleck and Sridhar observed shear crimping failure. To determine whether shear crimping (shear buckling) is a member or localised type of buckle, buckling tests on low slenderness - short sandwich columns identified as possibly exhibiting shear crimping were performed. This paper presents the

results of global buckling tests on sandwich columns under compression with low slenderness.

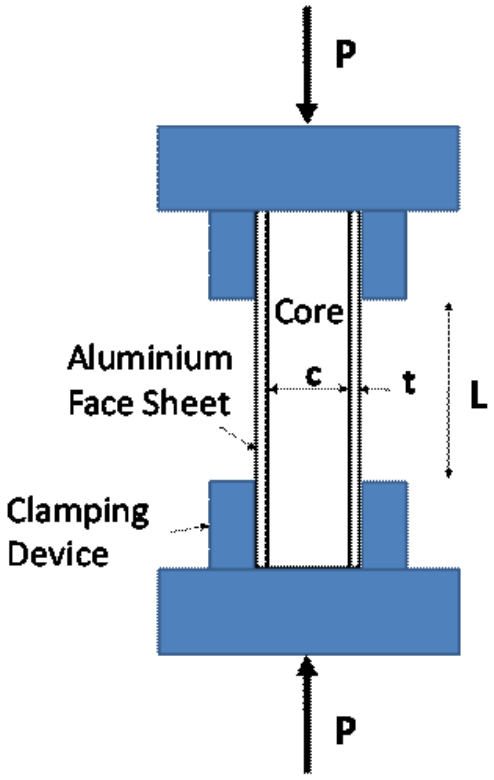

Figure 2 Fixed End Sandwich Column under Compression

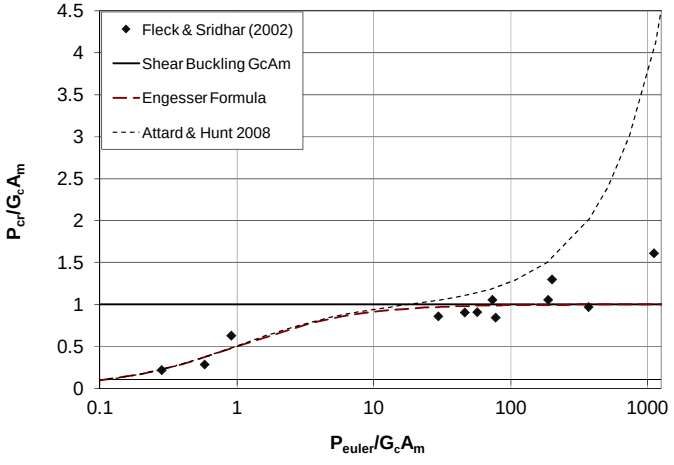

Figure 3 Experimental Results on Sandwich Columns

2 REVIEW OF COLUMN AND SANDWICH COLUMN BUCKLING EQUATIONS

Here we review the derivations for the global buckling load of a prismatic column made of an isotropic material under compression with shear deformations included. The beam centroidal axis is taken as the x axis while the vertical principal axis is taken as the y axis. The bending equilibrium equation is then:

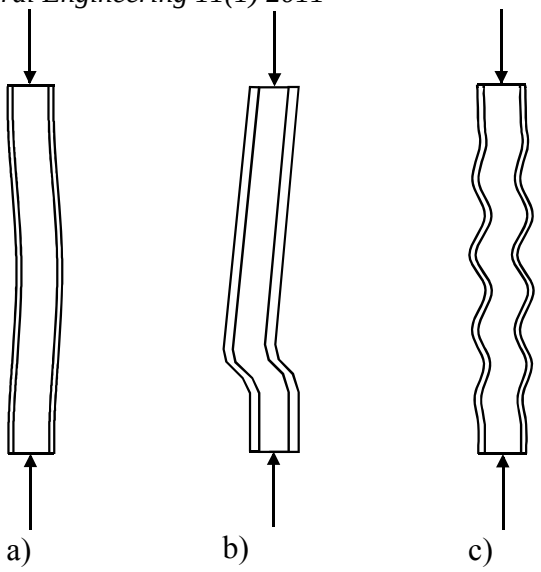

Figure 4 Sandwich Column Buckling Modes a) Euler Buckling
b) Shear Crimping
c) Face Sheet Wrinkling

$$M = P_x v + P_y\left(x + u_o\right) + M_o$$
$$\frac{dM}{dx} = P_x\frac{dv}{dx} + P_y\left(1 + \frac{du_o}{dx}\right) = -Q_t \qquad (6)$$

With v being the vertical deflection of centroidal axis, u_o the axial displacement of the centroid, M the bending moment, Q_t the shear force perpendicular to centroidal axis and, P_x and P_y are the force resultants at a cross-section in the x and y directions, respectively. For a statically determinate simply supported beam under end compression P, the force resultants would be P_x=-P and P_y=0. Substituting the curvature bending constitutive relationship into Eq. (6) and differentiating twice gives

$$EI\frac{d\theta}{dx} = P_x v + P_y\left(x + u_o\right) + M_o$$
$$EI\frac{d^2\theta}{dx^2} + P\frac{dv}{dx} = 0 \;\rightarrow EI\frac{d^2\theta}{dx^2} + P\left(\theta + \varphi\right) = 0 \qquad (7)$$

Where EI is the bending rigidity, θ is the bending rotation of the cross-section and φ is the shear rotation. The shear constitutive relationship is different in the Engesser and Haringx models. Haringx takes the shear force as parallel to the cross-section while Engesser takes the shear force as tangential to the centroidal axis. The shear constitutive relationships are therefore:

$$GA\varphi - P\theta = 0 \quad \therefore \varphi = \frac{P\theta}{GA} \qquad \text{Haringx} \quad (8)$$

$$GA\varphi - P\left(\theta + \varphi\right) = 0 \quad \therefore \varphi = \frac{P\theta}{GA - P} \qquad \text{Engesser} \quad (9)$$

The boundary conditions for the simply supported column of length L are $EI\frac{d\theta}{dx}=0\,(x=0,L)$. Note the boundary conditions and shear constitutive equation imply $\frac{d\varphi}{dx}=0\,(x=0,L)$. Solving the buckling problem using Eqs (7) to (9) gives

$$\frac{P_{cr\_Eng}}{GA}=\frac{\frac{P_{euler}}{GA}}{1+\frac{P_{euler}}{GA}} \qquad \frac{P_{cr\_Har}}{GA}=\frac{1}{2}\left(\sqrt{1+\frac{4P_{euler}}{GA}}-1\right) \tag{10}$$

If we include the effects of the axial deformation prior to buckling as detailed in [7], the buckling formulas would be:

$$\begin{aligned}\frac{P_{cr\_Eng2}}{EA}&=\frac{1}{2}\left(1\pm\sqrt{1-\frac{4P_{cr\_Eng}}{EA}}\right)\\ \frac{P_{cr\_Har2}}{EA}&=\frac{1}{2\left(1-\frac{E}{G}\right)}\left(1\pm\sqrt{1-\frac{4P_{euler}}{EA}\left(1-\frac{E}{G}\right)}\right)\end{aligned} \tag{11}$$

Reference [7] also gives the second variation of the total potential based on the Engesser and Haringx approaches:

$$\tfrac{1}{2}\int_0^L\left[EI_{zz}\left(\theta_{,x}\right)^2-P\left(v_{,x}\right)^2+GA(\varphi)^2\right]dx \quad Engesser \tag{12}$$

$$\tfrac{1}{2}\int_0^L\left[EI_{zz}\left(\theta_{,x}\right)^2-P\left(v_{,x}\right)^2+\{GA+P\}(\varphi)^2\right]dx \; Haringx \tag{13}$$

Here we now compare the second variation of the total potential for a sandwich column with a weak core with that for the column made of one isotropic material. For a weak core, a zig-zag type displacement is assumed with the face sheets shearing with respect to the core as shown in Figure 5. The internal actions are separated into those acting on the face sheets and those acting on the core as in Figure 5b). The bending of the face sheet plane is denoted by the angle θ_f while the shear angle of the face sheet is denoted by φ_f (see Figure 5). The rotation of the mid-plane of the face sheet is the sum of the rotations $\theta_f+\varphi_f$. The core cross-sectional plane rotates θ_c from the vertical while the shear of the core is defined by

$$\varphi_c=\theta_f+\theta_c+\varphi_f \tag{14}$$

The bending rotations θ_f, θ_c and shear angles φ_c, φ_f are all assumed to be functions of the longitudinal coordinate x, only. As shown in [7], the slope of the centroidal axis is given by:

$$\frac{dv}{dx}=\theta_f+\varphi_f \tag{15}$$

Reference [7] derives the second variation of total potential for the sandwich column using a hyperelastic constitutive model and an approach consistent with Haringx's approach, that is:

$$\tfrac{1}{2}\int_0^L\left[\begin{array}{l}EA_{tot}\left(\delta u_{o,x}\right)^2+EI_{tot}\left(\delta\theta_{f,x}\right)^2\\ +r_{c2}^2EA_{tot}\left(\delta\varphi_{c,x}-\delta\varphi_{f,x}\right)^2\\ -2r_c^2EA_{tot}\left(\delta\varphi_{c,x}-\delta\varphi_{f,x}\right)\delta\theta_{f,x}\\ -P\left(1-\bar{P}\right)\left(\delta\theta_f+2\delta\varphi_f\right)\delta\theta_f\\ +\left\{2G_fA_f\left(1-\bar{P}\right)+N_c\right\}\left(1-\bar{P}\right)\left(\delta\varphi_f\right)^2\\ +\left\{G_cA_c\left(1-\bar{P}\right)-N_c\right\}\left(1-\bar{P}\right)\left(\delta\varphi_c\right)^2\end{array}\right]dx \tag{16}$$

Where $\bar{P}=\frac{P}{EA_{tot}}$ and N_c is the axial force taken by the core. For the case when the shear deformation in the face sheet, the axial deformation prior to buckling and the axial deformation terms are ignored, the second variation of work simplifies to:

$$\tfrac{1}{2}\int_0^L\left[\begin{array}{l}EI_{tot}\left(\delta\theta_{f,x}\right)^2+r_{c2}^2EA_{tot}\left(\delta\varphi_{c,x}\right)^2\\ -2r_c^2EA_{tot}\delta\varphi_{c,x}\delta\theta_{f,x}\\ -P\left(\delta\theta_f\right)^2+\left\{G_cA_c-N_c\right\}\left(\delta\varphi_c\right)^2\end{array}\right]dx \tag{17}$$

Now if we further assume that the face sheets are so thin that $t<<c$ then from Eqn (4) we have

$$r_c^2\approx r^2-\frac{2E_fI_f}{EA_{tot}}\approx r_{c2}^2=\frac{E_cI_c+2E_fA_f\left(\frac{c}{2}\right)^2}{EA_{tot}} \tag{18}$$

Hence Eq. (17) becomes

$$\tfrac{1}{2}\int_0^L\left[\begin{array}{l}2E_fI_f\left(\delta\theta_{f,x}\right)^2-P\left(\delta\theta_f\right)^2\\ +\left(E_cI_c+2E_fA_f\left(\frac{c}{2}\right)^2\right)\left(\delta\theta_{f,x}-\delta\varphi_{c,x}\right)^2\\ +\left\{G_cA_c-N_c\right\}\left(\delta\varphi_c\right)^2\end{array}\right]dx \tag{19}$$

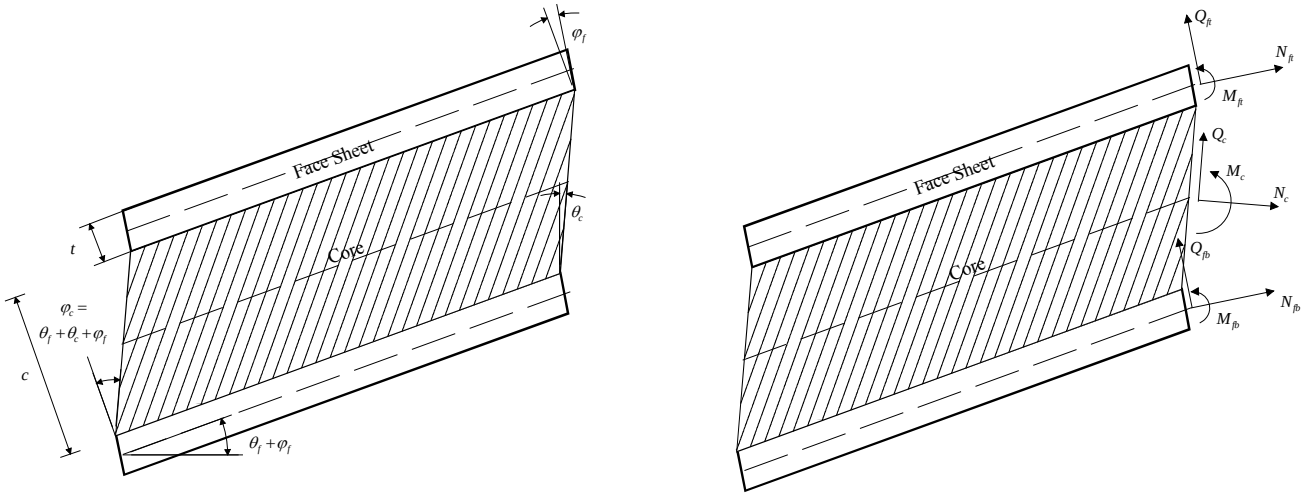

a) Displacements b) Internal actions

Figure 5 Sandwich Column Displacements and Internal Actions

If the axial force in the core is now ignored and for no shear within the face sheet we note $\frac{dv}{dx} = \theta_f$ then Eq (19) becomes:

$$\frac{1}{2}\int_0^L \left[\begin{array}{l} 2E_f I_f \left(\delta\theta_{f,x}\right)^2 - P\left(\delta v_{,x}\right)^2 + G_c A_c \left(\delta\varphi_c\right)^2 \\ + \left(E_c I_c + 2E_f A_f \left(\frac{c}{2}\right)^2 \right)\left(\delta\theta_{f,x} - \delta\varphi_{c,x}\right)^2 \end{array} \right] dx \quad (20)$$

From Eq (14), $\theta_c = \varphi_c - \theta_f$ and is the bending rotation of the core. Equation (20) further reduces to:

$$\frac{1}{2}\int_0^L \left[\begin{array}{l} 2E_f I_f \left(\delta\theta_{f,x}\right)^2 - P\left(\delta v_{,x}\right)^2 + G_c A_c \left(\delta\varphi_c\right)^2 \\ + \left(E_c I_c + 2E_f A_f \left(\frac{c}{2}\right)^2 \right)\left(\delta\theta_{c,x}\right)^2 \end{array} \right] dx \quad (21)$$

Except for the flange bending term $2E_f I_f \left(\delta\theta_{f,x}\right)^2$, the above expression is similar to the second variation of total potential for the column buckling problem using Engesser's approach, Eq.(12). Consider the simply supported case and assume:

$$v = v_m \sin\left(\frac{\pi x}{L}\right) \quad \theta_f = \frac{\pi v_m}{L}\cos\left(\frac{\pi x}{L}\right)$$
$$\varphi_c = \varphi_m \cos\left(\frac{\pi x}{L}\right) \quad (22)$$

Where v_m is the vertical displacement at the midspan and φ_m is the shear rotation at support x=0. Then substituting into Eq. (21), we can solve for the buckling load, which is:

$$\frac{P_{cr}}{G_c A_c} = \frac{P_{face}}{G_c A_c} + \frac{\frac{P_{euler}}{G_c A_c} - \frac{P_{face}}{G_c A_c}}{1 + \frac{P_{euler}}{G_c A_c} - \frac{P_{face}}{G_c A_c}} \quad (23)$$

This is the same as Allen's equation for thick faces if A_m is substituted for the area of the core A_c.

3 TEST SPECIMENS AND MATERIAL PROPERTIES

Sandwich columns were constructed for testing in compression according to ASTM C 364-99 [1]. Figures 1 and 4 shows a typical column loaded in compression while being clamped at both ends. The sandwich column test specimens were constructed from Divinycell H45, H80, H100 and H200 foam for the core and face sheets made of Aluminium 2024-T3. The lengths of the columns varied from 20 to 500 mm. For each foam type and sample length, two sandwich columns were produced. The clear spans of the columns were 20, 30, 40, 50, 75 100, 200 and 500 mm. The length of the clamps in the testing rig was 22mm at each end. For each specimen, the width of the face sheets was 100 mm. The core thickness was 10.5 mm, while the face thickness was 1 mm.

Measurements of the mid-span lateral displacement were used in a Southwell type plot to determine the elastic buckling load. The shear modulus of the core was determined from three point bending tests according to ASTM-C-393 [2]. Specimens were made from cutting the aluminium sheets and foam cores into the required size using a saw.

The aluminium face sheets were abraded using sandpaper and cleaned using acetate acid prior gluing. The adhesive chosen was a rubber-toughened epoxy, trade name "Devcon Epoxy Plus". This epoxy was chosen for its high tensile shear strength, high tensile-peel strength, and for its ability to bond dissimilar substrates. High peel strength is essential for composite materials as there is high strength demand in the adhesive during loading. If the adhesive peel strength is low, then the face sheets will delaminate from the foam core.

The epoxy adhesive was applied to the facesheets and core and let dry for one minute. This allowed the epoxy adhesive to fully bond. The facesheets were glued onto the foam cores and pressed together using weights. The weight used during curing was approximately 170 kgs/m2. The weights remained on the specimens for approximately 48 hours. The specimens were cured for at least 7 days prior to testing.

The columns were end-clamped according to ASTM C 364-99 [1] and placed in a servo-controlled compression testing machine (see Figure 2). The specimens were compressed axially at different displacement rates depending on the foam density. The displacement rates were 0.50 mm s^{-1}, 0.40 mm s^{-1}, 0.25 mm s^{-1} and 0.15 mm s^{-1} for H200, H100, H80 and H45 respectively. The specimens were compressed at a constant rate until the specimens failed. The applied load and cross-head displacement was measured using the load cell of the testing machine. The net lateral deflection of the column mid-height was recorded using two linear variable differential transformers (LVDT).

Table 1 Shear Modulus G_c (MPa)

	H45	H80	H100	H200
Test Results	13	21	31	57
Manufacturer [27]	15 (12)	27 (23)	35 (28)	85 (75)

Manufacturer's values are average values for the nominal densities and within the brackets minimum values for the minimum density

Three standard tensile specimens were cut from the supplied aluminium and tested in tension. The stress strain curve for the 2024-T3 Aluminium is shown in Figure 6. The nominal proportional limit was 310 MPa while the elastic modulus was 68800 MPa. The shear modulus of the Divinycell cores was determined from three point bending tests according to ASTM-C-393 [2]. The results for the shear modulus for the Divinycell cores are compared to the manufacturer's guide [27] in Table 1. It is noted that generally the measured shear modulus was close to the manufacturer's guide expect for the H200.

4 TEST RESULTS

The average measured lateral deflection Δ at mid-height was used to plot a Southwell Plot, see reference [28]. The Southwell is a nondestructive procedure for estimating the buckling load. The Southwell plot is a plot of Δ/P versus Δ. The reciprocal of the slope of the linear portion of the Southwell plot gives an estimate of the buckling load. Table 2 gives the estimated buckling loads using the Southwell Plot and the peak loads. Figure 7 gives a plot of the peak loads versus the Southwell estimate. The predictions based on the Southwell Plot are consistent with the peak loads. Figure 7 gives a plot of the peaks load versus the corresponding Southwell Plot prediction. The mean difference is approximately +5%. Table 3 contains the estimated normal stress range in the face sheets based on the peak axial load and the stress caused by the lateral bending moment calculated from the average lateral displacement at mid-span (ignoring the fixed end moment within the clamp). The stress range above the proportional limit of 310 MPa for the aluminum face sheets, are highlighted. Generally the buckled shape was an Euler type buckle. For the very short columns of lengths 20 and 30, the Euler buckle was coupled with buckling of one of the faces within the clamped zone.

Figures 7-10 shows the load versus lateral displacement plots for columns of length 20, 40, 100 and 500 mm. It can be seen that there is a significant softening of the load carrying capacity in the post-buckling region for the shorter columns. Figures 11 and 12 are plots of the normalized buckling load, P_{cr}/G_cA_m based on the peak load, against either the column length or the normalized parameter, P_{euler}/G_cA_m. Also plotted in Figure 12 is the elastic limit based on a proportional limit stress of 310 MPa in the face sheets. Figures 11 and 12 do not show an upper limit of G_cA_m the shear crimping or shear buckling load. The peak load for the very short columns has a maximum of approximately $3.2G_cA_m$, well above the shear crimping limit. The results generally follow the predictions of Eq. (5) except for some of the very short specimens whose failure load was close to the proportional limit of the face sheet or where there was buckling of the face sheets with-

in the clamped zone. There was no shear crimping or shear buckling mode type failures.

5 SUMMARY

The buckling formulas, theoretical approaches and definition for beam internal force actions of Engesser and Haringx for isotropic columns and soft shear core sandwich columns were detailed and reviewed. A important distinction is made between the isotropic single material column buckling formula attributed to Haringx and the theoretical assumptions underpinning his approach. Haringx's single isotropic material column buckling formula is not applicable to sandwich columns or to laced columns, columns with batten plates or with perforated cover plates and columns with open webs, where there is a zig-zag shearing pattern of deformations through the cross-section. This does not mean that Haringx's theoretical approach and that of Reissner cannot be used for sandwich columns. Problems occur when a sandwich column with two materials (face sheet and core) is modeled by an equivalent column with a single effective bending and shear rigidity. In this paper it was shown that the theoretical approaches of Haringx and Engesser yield the same buckling formula for soft shear core sandwich columns when the thickness is very small in comparison to the core thickness, and the shear in the face sheets, the axial force in the core and the bending within the face sheets are ignored.

To determine whether a shear crimping or shear buckling upper limit exists for sandwich columns, elastic buckling tests were performed on sandwich columns constructed from 10 mm thick Divinycell H45, H80, H100 and H200 foam for the core and 1 mm face sheets made of Aluminum 2024-T3. The lengths of the columns varied from 20 to 500 mm. The columns were end-clamped according to ASTM C 364-99 [1] and placed in a servo-controlled compression testing machine. The width of the specimens was 100 mm and two specimens at each length were tested. Measurements of the mid-span lateral displacement were used in a Southwell type plot to determine the elastic buckling load. The shear modulus of the core was determined from three point bending tests according to ASTM-C-393 [2]. In the tests carried out, some of the very short specimens failed with buckling of the face sheet within the clamped region. None of the tests exhibited shear crimpling or shear buckling modes and the buckling loads for very short columns were much higher than the shear buckling limit of Engesser G_cA_m. When the slenderness is very small, the buckling load of the face sheets acting independently dominates unless there is failure activated by material failure. We would therefore not expect to see shear buckling and none were observed in the presented experiments.

Table 2 Experimental Results for Buckling Load

L (mm)	Pcr (kN) Peak Load				Pcr (kN) Southwell Plat			
	H45	H80	H100	H200	H45	H80	H100	H200
20	52.5	56.3	*65.7**		60.2	58.8	*69.0**	
20	38.4	50.4	*68.7**		42.2	55.6	*73.5**	
30	39.1	56	*61.8**		41.1	61.3	*60.6**	
30	42.9	57.2	60.5		47.9	63.7	57.8	
40	40.5	54.8	59.2		41.7	62.1	55.9	
40	32.1	47.1	58.6		42.2	49.8	58.8	
50	25.4	49.4	38.4		27.8	52.9	34.8	
50			47.5				52.1	
75	25.3	38.5	52.2		28.0	39.5	52.6	
75	17.4	35.5	50.4		17.5	38.3	50.5	
100	18.9	28.1	37.3	*67.7**	19.3	35.6	37.7	*67.7**
100	21.1	34.3	43.3	*68.6**	21.2	33.5	37.6	*70.4**
200	15.7	21.3	25.1	45.6	16.9	23.3	27.8	51.5
200	17.5	16.4	36.7	*46.0**	18.2	18.2	40.0	*52.4**
500	9.2	21.7	21.5	*34.7**	10.8	22.7	23.3	*37.0**
500	11.2	19.1	18.7	*28.9**	12.3	19.6	21.3	*32.3**

* Stresses above proportional limit

REFERENCES

Allen, H.G., *Analysis and Design of Structural Sandwich Panels*. 1969, Oxford: Pergamon.

Aristizabal-Ochoa, J., *Slope-deflection equations for stability and second-order analysis of Timoshenko beam–column structures with semi-rigid connections.* Engineering Structures, 2008. 30(11): p. 3394-3395.

ASTM-C-364-99, *Standard Test Method for Edgewise Compressive Strength of Sandwich Constructions*, in *Vol. 15.03*. 2000.

ASTM-C-393-00, Standard Test Method for Flexural Properties of Sandwich Constructions, in Vol. 15.03. 2000.

Attard, M.M. and G.W. Hunt, *Column Buckling with Shear Deformations - A Hyperelastic Formulation.* International Journal of Solids and Structures, 2008. 45(14-15): p. 4322-4339.

Attard, M.M. and G.W. Hunt, *Sandwich Column Buckling - A Hyperelastic Formulation.* International Journal of Solids and Structures, 2008. 45(21): p. 5540-5555.

Attard, M.M., *Extrapolation Techniques for Buckling Loads.* Journal of Structural Engineering, 1983. 109(4): p. 926-935.

Attard, M.M., *Finite Strain - Beam Theory.* International Journal Of Solids and Structures, 2003. 40(17): p. 4563-4584.

Attard, M.M., J.S. Lee, and M.Y. Kim, *Dynamic stability of shear-flexible beck's columns based on Engesser's and Haringx's buckling theories.* Computers and Structures, 2008. 86(21-22): p. 2042-2055.

Bažant, Z.P. and A. Beghini, *Sandwich buckling formulas and applicability of standard computational algorithm for finite strain.* Composites: Part B, 2004. 35: p. 573-581.

Bažant, Z.P. and A. Beghini, *Stability and finite strain of homogenized structures soft in shear: Sandwich or fiber composites, and layered bodies.* International Journal of Solids and Structures, 2006. 43: p. 1571-1593.

Bažant, Z.P. and L. Cedolin, *Stability of Structures*. 1991, New York: Oxford University Press, Inc.

Bažant, Z.P., *Shear Buckling of Sandwich, Fiber-Composite and Lattice Columns, Bearings and Helical Springs: Paradox Resolved.* ASME Journal of Applied Mechanics, 2003. 70 p. 75-83.

Bazant, Z.P., *Structural stability.* International Journal of Solids and Structures, 2000. 37(1-2): p. 55-67.

Beghini, A., et al., *Initial postcritical behavior of sandwich columns with low shear and transverse stiffness.* Composites Part B, 2008. 39(1): p. 159-164.

Blaauwendraad, J., *Timoshenko beam–column buckling. Does Dario stand the test?* Engineering Structures, 2008. 30(11): p. 3389-3393.

DIAB, *Divinycell H Technical Manual*. 2007.

Engesser, F., *Die Knickfestigkeit gerader St be.* Zeitschrift des Architekten und Ingenieur Vereins zu Hannover, 1889. 35: p. 455.

Engesser, F., *Die Knickfestigkeit gerader St be.* Zeutralblatt des Bauverwaltung, 1891. 11: p. 483.

Fleck, N.A. and L. Sridhar, *End Compression of Sandwich Columns.* Composites, Part A: Applied Science and Manufacturing, 2002. 33: p. 353-359.

Gjelsvik, A., *Stability of Built-Up Columns.* Journal of Engineering Mechanics, ASCE, 1991. 117(6, June): p. 1331-1345.

Haringx, J.A., *On the Buckling and Lateral Rigidity of Helical Springs.* Proc. Konink. Ned. Akad. Wet.,, 1942. 45: p. 533.

Kardomateas, G.A. and D.S. Dancila, *Buckling of Moderately Thick Orthotropic Columns: Comparsion of an Elasticity Solution with the Euler and Engesser/Haringx/Timoshenko Formulae.* International Journal of Solids and Structures, 1997. 34(3): p. 341-357.

Reissner, E., *Some Remarks on the Problem of Column Buckling.* Ingenieur-Archiv, 1982. 52: p. 115-119.

Simo, J.C., K.D. Hjelmstad, and R.L. Taylor, *Numerical Formulations of Elasto-Viscoplastic Response of Beams Accounting for the Effect of Shear.* Computer Methods in Applied Mechanics and Engineering, 1984. 42: p. 301-330.

Timoshenko, S.P. and J.M. Gere, *Theory of Elastic Stability*. 1963: McGraw-Hill International London.

Vadakke, V. and L.A. Carlsson, *Experimental Investigation of Compression Failure Mechanisms of Composite Faced Foam Core Sandwich Specimens.* Journal of Sandwich Structures and Materials, 2004. 6(July): p. 327-342.

Zielger, H., *Arguments For and Against Engesser's Buckling Formulas.* Ingenieur-Archiv, 1982. 52: p. 105-113.

Table 3 Face Sheet Normal Stress Range

L (mm)	Face Sheet Normal Stress Range (MPa)			
	H45	H80	H100	H200
20	261-262	281-300	*328-347**	
20	191-194	251-260	*342-354**	
30	195-204	279-296	*308-320**	
30	214-229	285-289	301-306	
40	202-202	273-282	295-301	
40	160-169	235-247	292-298	
50	127-139	246-254	191-193	
50			237-237	
75	126-138	192-211	260-271	
75	87-91	177-197	251-264	
100	94-105	140-160	186-211	*337-363**
100	105-110	171-178	216-220	*342-364**
200	79-104	106-135	125-169	227-246
200	87-98	82-109	183-231	*229-332**
500	46-108	108-156	107-194	*173-332**
500	56-86	95-175	93-181	*144-300**

* Stresses above proportional limit

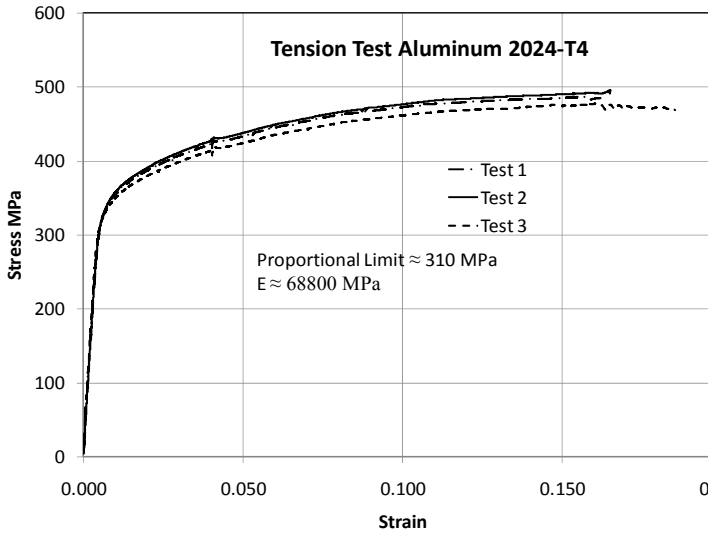

Figure 6 Tensile Stress Strain Curve for 2024-T3 Aluminium

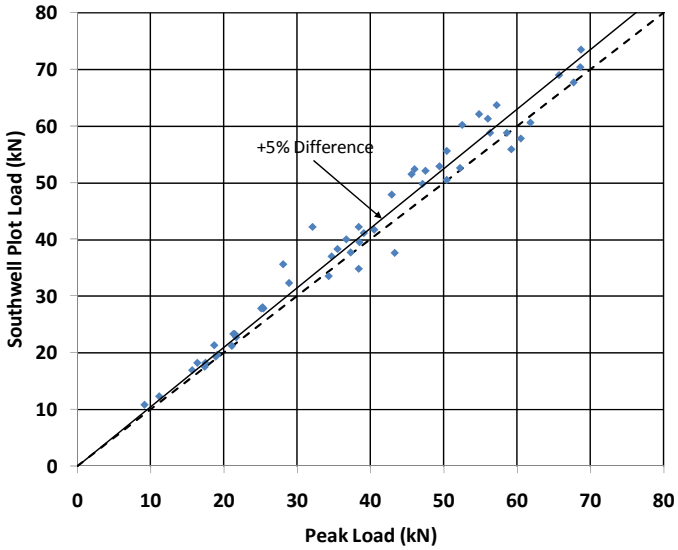

Figure 7 Comparison between Peak Load and Southwell Plot Estimate

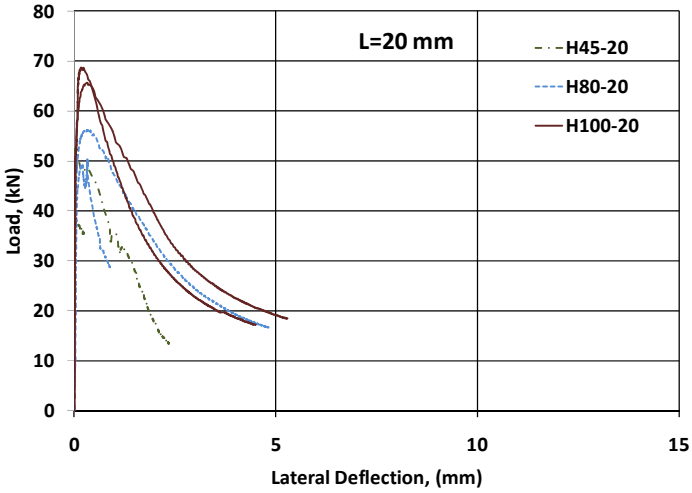

Figure 8 Load versus Lateral Deflection for 20mm Columns

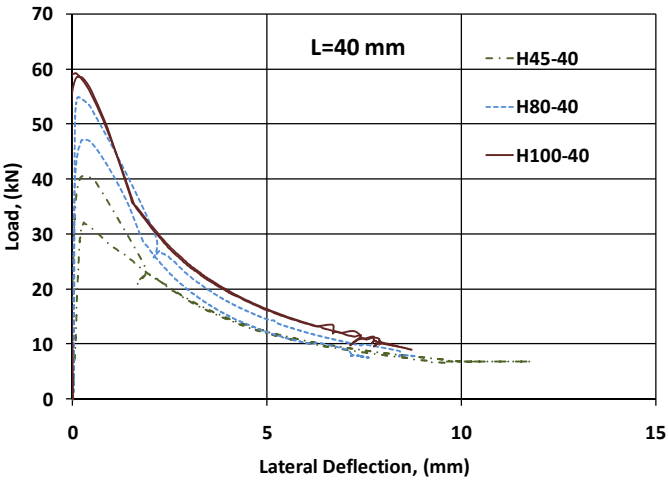

Figure 9 Load versus Lateral Deflection for 40mm Columns

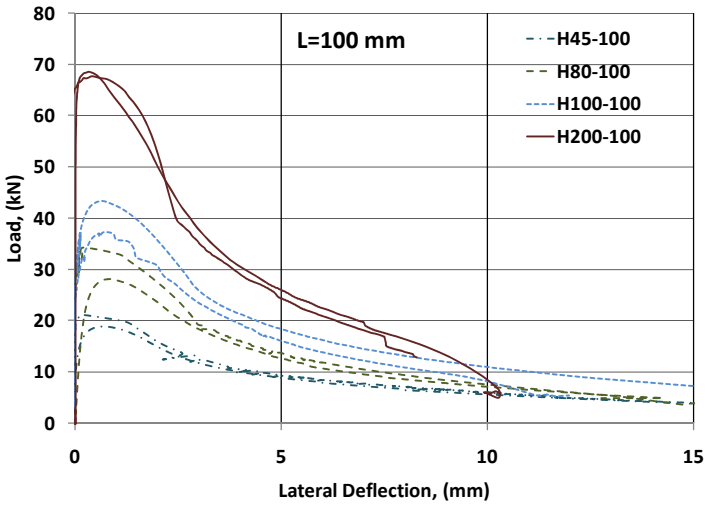

Figure 10 Load versus Lateral Deflection for 100mm Columns

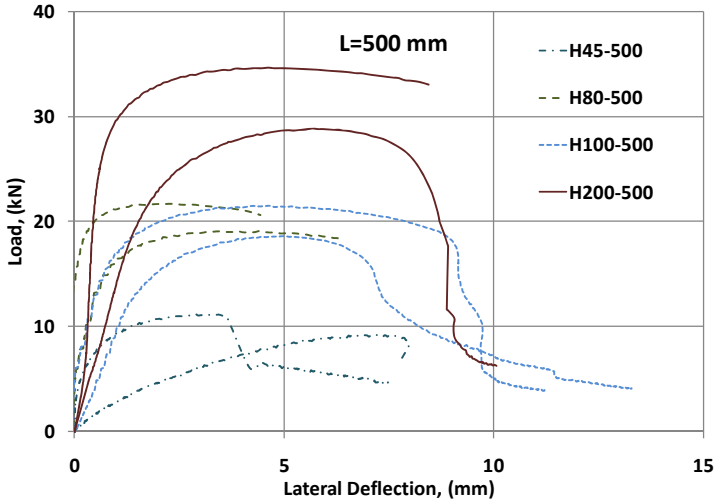

Figure 11 Load versus Lateral Deflection for 500mm Columns

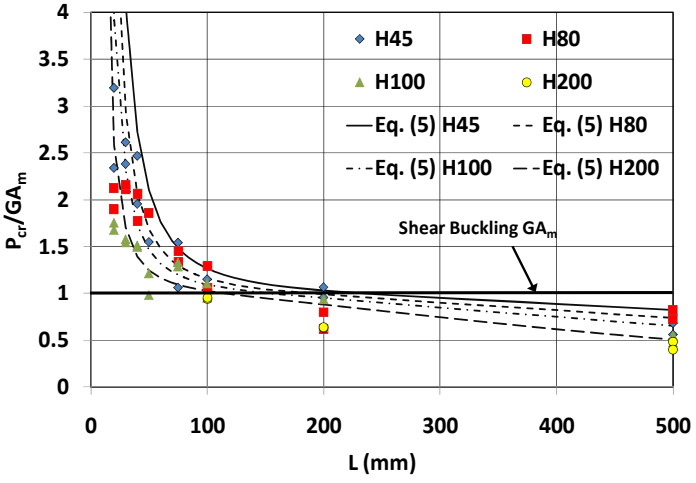

Figure 12 Comparison of the Experimental Peak Loads with Attard & Hunt [11] Eq. (5)

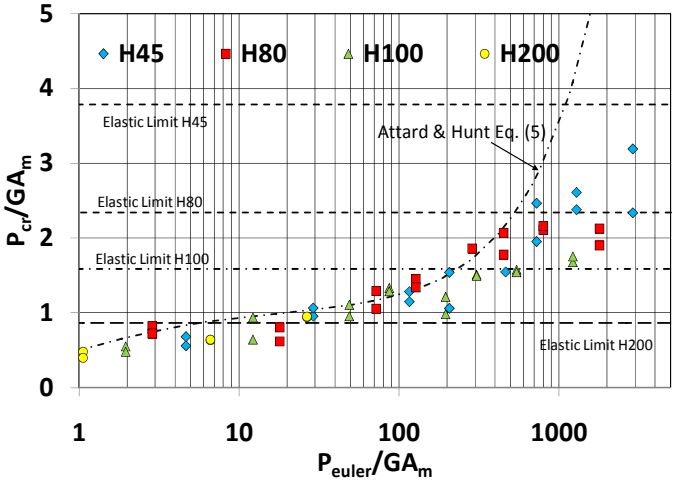

Figure 13 Comparison of the Experimental Peak Loads Attard & Hunt [11] Eq. (5)